

CrossMark  
click for updatesCite this: *Chem. Sci.*, 2015, 6, 7201

# A recyclable polyoxometalate-based supramolecular chemosensor for efficient detection of carbon dioxide†

Haibing Wei,<sup>ab</sup> Jinlong Zhang,<sup>a</sup> Nan Shi,<sup>a</sup> Yang Liu,<sup>a</sup> Ben Zhang,<sup>a</sup> Jie Zhang<sup>\*a</sup> and Xinhua Wan<sup>\*a</sup>

A new type of supramolecular chemosensor based on the polyoxometalate (POM) Na<sub>9</sub>DyW<sub>10</sub>O<sub>36</sub> (DyW<sub>10</sub>) and the block copolymer poly(ethylene oxide-*b*-*N,N*-dimethylaminoethyl methacrylate) (PEO<sub>114</sub>-*b*-PDMAEMA<sub>16</sub>) is reported. By taking advantage of the CO<sub>2</sub> sensitivity of PDMAEMA blocks to protonate the neutral tertiary amino groups, CO<sub>2</sub> can induce the electrostatic coassembly of anionic DyW<sub>10</sub> with protonated PDMAEMA blocks, and consequently trigger the luminescence chromism of DyW<sub>10</sub> due to the change in the microenvironment of Dy<sup>3+</sup>. The hybrid complex in dilute aqueous solution is very sensitive to CO<sub>2</sub> content and shows rapid responsiveness in luminescence. The luminescence intensity of the DyW<sub>10</sub>/PEO-*b*-PDMAEMA complex increases linearly with an increasing amount of dissolved CO<sub>2</sub>, which permits the qualitative and quantitative detection of CO<sub>2</sub>. The complex solution also shows good selectivity for CO<sub>2</sub>, with good interference tolerance of CO, N<sub>2</sub>, HCl, H<sub>2</sub>O and SO<sub>2</sub>. The supramolecular chemosensor can be recycled through disassembly of the hybrid complex by simply purging with inert gases to remove CO<sub>2</sub>.

Received 5th June 2015

Accepted 3rd September 2015

DOI: 10.1039/c5sc02020d

www.rsc.org/chemicalscience

## Introduction

Carbon dioxide (CO<sub>2</sub>) is a known greenhouse gas which is responsible for global climate change and also related to many human diseases, such as hypercapnia, hypocapnia and metabolic disorders, as well as being important in coalmine safety and volcanic activity.<sup>1</sup> CO<sub>2</sub> sensing and detecting is of great significance. For example, monitoring of dissolved CO<sub>2</sub> in arterial blood allows a timely clinical response in the case of patients with pneumonia or acute respiratory distress syndrome.<sup>2</sup> Nowadays, CO<sub>2</sub> detecting and sensing methods, including electrochemical systems,<sup>3</sup> near-infrared spectroscopic techniques,<sup>4</sup> gas chromatography<sup>5</sup> and optical chemosensors<sup>6</sup> are well-established. Among these, state-of-the-art Severinghaus-type electrochemical CO<sub>2</sub> sensors are widely used in commercial clinical blood gas analyzers, but these probes still suffer from a long response time and are only capable of detecting a relatively high CO<sub>2</sub> concentration, because their working performance relies on diffusion and the establishment

of an equilibrium between the internal pH electrode and the sample.<sup>7</sup> Alternatively, CO<sub>2</sub> chemosensor systems based on colorimetric and fluorimetric analysis take advantage of the outcome of chromism visible to the naked eye, which can be helpful for rapid on-site monitoring.<sup>8</sup> A few pH indicators or pH dependent fluorescent dyes have been used to produce such a type of optical sensor.<sup>6a,8c-e</sup> However, pH-dependent organic chromatic molecules that can simultaneously meet the needs of appropriate pK<sub>a</sub>, specificity, photostability, and contrast are very limited.

Supramolecular chemosensors are promising candidates to overcome the limitations of conventional optical chemosensors. Specially designed supramolecular chemosensors are fabricated by noncovalent binding between the molecular recognizer and the molecular reporter, and the sensing works by a relay mechanism:<sup>9</sup> the recognizer detects the analyte, then communicates with the reporter by physical or chemical means, and eventually the optical signals of the reporter are switched on. This strategy integrates the complementary functions of multiple components, and is advantageous for CO<sub>2</sub> sensing in that it greatly expands the options of chromatic molecules and improves sensitivity and stability. In addition, by taking advantage of the dynamic nature of the noncovalent binding of supramolecular systems, device recyclability can be achieved, which is crucial for low cost and environmental concerns. Tang *et al.*<sup>8b</sup> developed a CO<sub>2</sub> sensor based on a fluorogen with aggregation-induced emission in dipropylamine. Besides this, supramolecular CO<sub>2</sub> sensors are still rare and it is a challenge to

<sup>a</sup>Beijing National Laboratory for Molecular Sciences, Key Laboratory of Polymer Chemistry and Physics of Ministry of Education, College of Chemistry and Molecular Engineering, Peking University, Beijing 100871, China. E-mail: jz10@pku.edu.cn; xhwan@pku.edu.cn

<sup>b</sup>School of Chemistry and Chemical Engineering, Provincial Key Laboratory of Advanced Functional Materials and Devices, Hefei University of Technology, Hefei, Anhui 230009, China

† Electronic supplementary information (ESI) available. See DOI: 10.1039/c5sc02020d

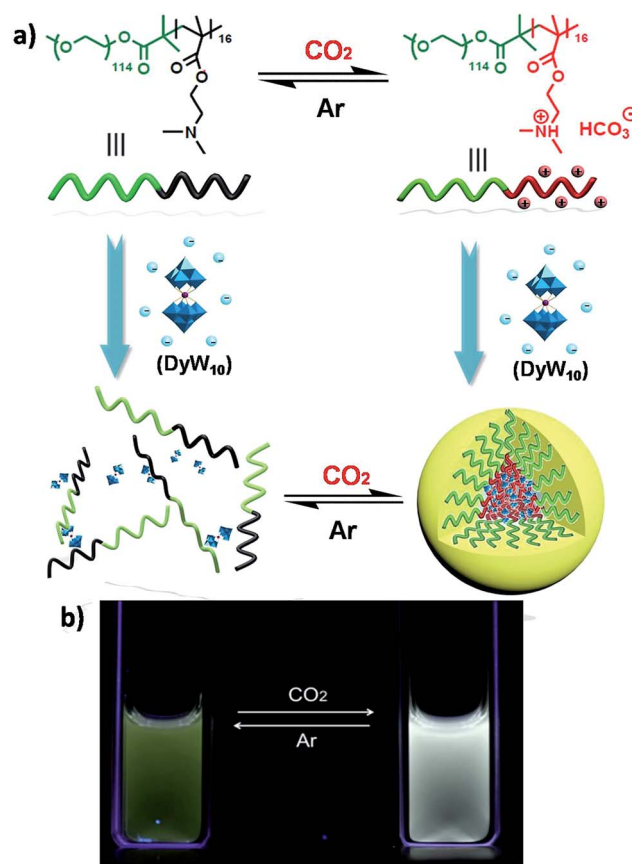


elaborately construct a supramolecular system for CO<sub>2</sub> detection with the characteristics of high sensitivity, low detection limit, specificity, photostability, and recyclability.

Recently we have discovered hybrid supramolecular systems with the variable luminescence properties of lanthanide-containing polyoxometalates (POMs) by coacervate complexation with block polyelectrolytes.<sup>10</sup> The lanthanide-containing polyoxometalates possess excellent photoluminescent properties, *i.e.* narrow emission bands, large Stokes shifts, long lifetimes and photostability, and are sensitive to ambient chemical environments.<sup>11</sup> The dysprosium-containing POM Na<sub>9</sub>DyW<sub>10</sub>O<sub>36</sub> (DyW<sub>10</sub>) has two characteristic emission bands, *viz.*, <sup>4</sup>F<sub>9/2</sub> → <sup>6</sup>H<sub>15/2</sub> (blue emission, λ<sub>em</sub><sup>max</sup> = 476 nm) and <sup>4</sup>F<sub>9/2</sub> → <sup>6</sup>H<sub>13/2</sub> (yellow emission, λ<sub>em</sub><sup>max</sup> = 574 nm) transitions, and their relative intensity ratio  $I_{4F_{9/2} \rightarrow 6H_{13/2}}/I_{4F_{9/2} \rightarrow 6H_{15/2}}$  varies according to the surrounding microenvironment, which results in luminescence chromism.<sup>11a,12</sup> Although the luminescence of lanthanide-containing POMs is not sensitive to CO<sub>2</sub>, assembly approaches can effectively tune their emission colors and intensities, and therefore their characteristics are promising when employed as supramolecular sensors.<sup>13</sup> In the present work, we constructed a DyW<sub>10</sub>-based supramolecular chemosensor for CO<sub>2</sub> detection and quantitation in aqueous systems with high sensitivity and specificity, rapid response and recyclability. Unlike previous CO<sub>2</sub> chemosensors, which depend primarily on chromism of organic fluorogens at the molecular level, our supramolecular CO<sub>2</sub> sensor is based on hybrid core-shell assemblies composed of the block copolymer poly(ethylene oxide-*b*-*N,N*-dimethylaminoethyl methacrylate) (PEO<sub>114</sub>-*b*-PDMAEMA<sub>16</sub>) and DyW<sub>10</sub> in aqueous solution. By taking advantage of the CO<sub>2</sub> sensitivity of PDMAEMA blocks to protonate the neutral tertiary amino groups,<sup>14</sup> CO<sub>2</sub> can induce the electrostatic coassembly of anionic DyW<sub>10</sub> with protonated PDMAEMA blocks, and consequently trigger the luminescence chromism of DyW<sub>10</sub> due to the change in the microenvironment of Dy<sup>3+</sup> (Scheme 1a). The luminescence variation is closely related to the CO<sub>2</sub> content in solution, which can be used to quantitate dissolved CO<sub>2</sub>.

## Results and discussion

The DyW<sub>10</sub>/PEO-*b*-PDMAEMA complex was prepared by the addition of PEO-*b*-PDMAEMA to a dilute DyW<sub>10</sub> solution (0.2 mg mL<sup>-1</sup>, 9.8 mL), where the molar ratio of tertiary amino groups in PDMAEMA to DyW<sub>10</sub> was set as 13.5 (the charge ratio of DyW<sub>10</sub>/PDMAEMA ~1.0). Bubbling a small volume of CO<sub>2</sub> gas through the solution in as short a time as <1 minute caused a striking change in the emission of DyW<sub>10</sub> from weak green light to intense white light (Scheme 1b), while bubbling CO<sub>2</sub> into dilute DyW<sub>10</sub> solution for a long time did not cause a color change. The quantum yield of the DyW<sub>10</sub>/PEO-*b*-PDMAEMA complex increased from 0.78% to 2.10% after treatment with CO<sub>2</sub>, while the molar absorptivity was almost unchanged (~7.0 × 10<sup>3</sup> L mol<sup>-1</sup> cm<sup>-1</sup> on the basis of Na<sub>9</sub>DyW<sub>10</sub>O<sub>36</sub>). As a potential CO<sub>2</sub> sensor, the complex solution is very sensitive to dissolved CO<sub>2</sub> content and shows rapid responsiveness. To track the luminescence variation at low contents of dissolved CO<sub>2</sub>, a certain amount of saturated CO<sub>2</sub> aqueous solution (1.45 g L<sup>-1</sup> at 100



Scheme 1 (a) Structural change of the PEO-*b*-PDMAEMA block copolymer and schematic representation of the reversible formation of a hybrid micelle after the reaction with CO<sub>2</sub> in aqueous medium. (b) Photos taken under illumination with 254 nm UV light, representing the CO<sub>2</sub>-responsive luminescence chromism of the DyW<sub>10</sub>/PEO-*b*-PDMAEMA complex in aqueous solution before/after CO<sub>2</sub> sensing.

kPa and 25 °C) was directly added to the hybrid complex solution. *In situ* PL monitoring was conducted to investigate the sensing time of the CO<sub>2</sub>, and a substantial increase in the emission intensity was observed after only 30 s. As can be seen in Fig. 1a, the luminescence intensity of the DyW<sub>10</sub>/PEO-*b*-PDMAEMA complex increased linearly with increasing content of dissolved CO<sub>2</sub> with a correlation coefficient of 0.9956 (Fig. 1b). As the value of  $I_{4F_{9/2} \rightarrow 6H_{13/2}}/I_{4F_{9/2} \rightarrow 6H_{15/2}}$  decreased with increasing CO<sub>2</sub> concentration (Fig. S1†), the emission color gradually evolved from green to white, as could be seen with the naked eye. The detection limit of dissolved CO<sub>2</sub> was around 1.5 mg L<sup>-1</sup>. The DyW<sub>10</sub>/PEO-*b*-PDMAEMA sensor responds to dissolved CO<sub>2</sub> in the range 0–47.9 mg L<sup>-1</sup>, and the linear range can be extended by changing the initial concentration of the DyW<sub>10</sub>/PEO-*b*-PDMAEMA complex (Fig. S2†). Therefore, this photophysical characteristic of DyW<sub>10</sub>/PEO-*b*-PDMAEMA solution allows for the qualitative and quantitative detection of CO<sub>2</sub>. Moreover, upon exposure to air, atmospheric CO<sub>2</sub> (~300 ppm) can stimulate the luminescence variation of the DyW<sub>10</sub>/PEO-*b*-PDMAEMA complex system (Fig. S3†), further demonstrating its high sensitivity.



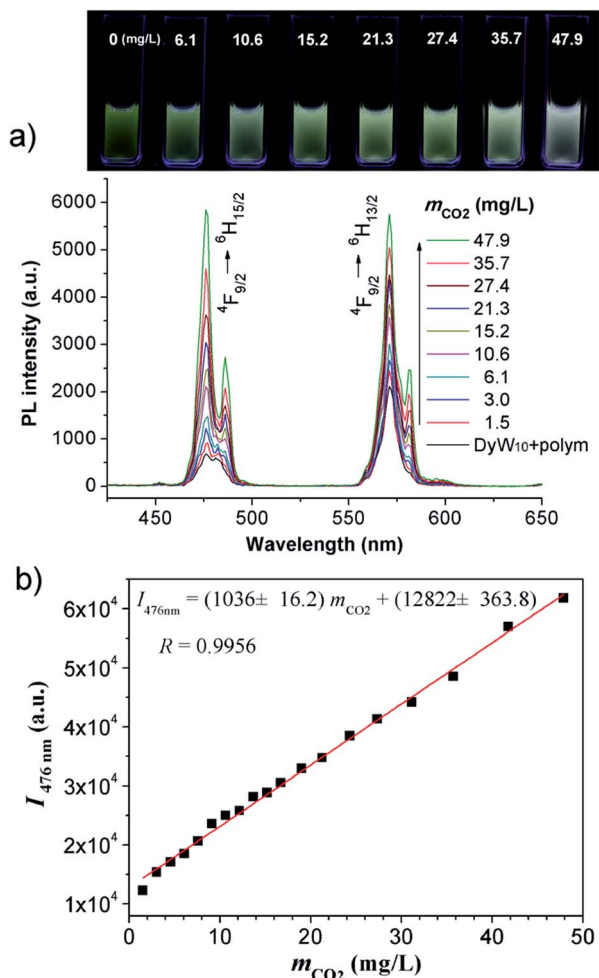


Fig. 1 (a) Variation in the PL spectra of DyW<sub>10</sub>/PEO-*b*-PDMAEMA hybrid complex (DyW<sub>10</sub>: 0.2 mg mL<sup>-1</sup>, 9.8 mL) in the presence of various concentrations of dissolved CO<sub>2</sub> at 25 °C (λ<sub>ex</sub> = 280 nm). Insert: photograph of DyW<sub>10</sub>/PEO-*b*-PDMAEMA hybrid complex in aqueous solution with different concentrations of dissolved CO<sub>2</sub> under UV illumination. (b) Plot of PL integrated intensities (blue emission, I<sub>4F<sub>9/2</sub>→<sup>6</sup>H<sub>15/2</sub></sub>) of the DyW<sub>10</sub>/PEO-*b*-PDMAEMA hybrid complex in aqueous solution as a function of dissolved CO<sub>2</sub> concentration at 25 °C (λ<sub>ex</sub> = 280 nm).

The complex solution shows good selectivity for CO<sub>2</sub>. CO, HCl, and SO<sub>2</sub> gases were purged into the solution. CO did not change the luminescence at all (Fig. S4<sup>†</sup>), while SO<sub>2</sub> quenched the luminescence because of the reduction of DyW<sub>10</sub> (Fig. S5<sup>†</sup>) and HCl gas also quenched the luminescence at low pH values (Fig. S6<sup>†</sup>) owing to the decomposition of DyW<sub>10</sub>. However, after purging with a mixed gas containing 20% CO<sub>2</sub>, 70% N<sub>2</sub>, 10% O<sub>2</sub> and 0.1% SO<sub>2</sub>, the complex solution still showed good detection of CO<sub>2</sub> (Fig. S7<sup>†</sup>), indicating that in practical applications CO, SO<sub>2</sub> and O<sub>2</sub> would not affect the CO<sub>2</sub> detection.

Furthermore, the sensor can be recycled by purging with inert gas to degas CO<sub>2</sub>. As shown in Fig. 2a, the emission spectrum of the complex solution after CO<sub>2</sub> treatment displays two intense blue and yellow bands, with an I<sub>4F<sub>9/2</sub>→<sup>6</sup>H<sub>13/2</sub></sub>/I<sub>4F<sub>9/2</sub>→<sup>6</sup>H<sub>15/2</sub></sub> value of ~0.92. After purging with Ar to degas CO<sub>2</sub>, the intensity strikingly decreased to the initial value

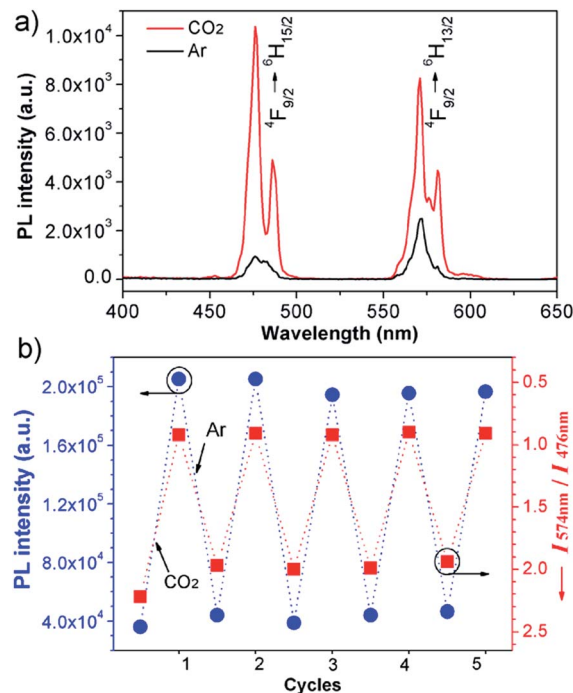


Fig. 2 (a) Emission spectra (λ<sub>ex</sub> = 280 nm) of DyW<sub>10</sub>/PEO-*b*-PDMAEMA coassembly in water before and after CO<sub>2</sub> treatment. (b) Reversible switching of the luminescence intensity and chromism of the DyW<sub>10</sub>/PEO-*b*-PDMAEMA solution by alternating CO<sub>2</sub>/Ar treatment.

before CO<sub>2</sub> treatment. I<sub>4F<sub>9/2</sub>→<sup>6</sup>H<sub>13/2</sub></sub>/I<sub>4F<sub>9/2</sub>→<sup>6</sup>H<sub>15/2</sub></sub> also increased to ~2.22, and correspondingly the emissive color recovered from strong white to the original weak green. Aside from Ar, the luminescence can be restored by purging with N<sub>2</sub> or simply heating, although the heating treatment takes longer (Fig. S8 and S9<sup>†</sup>). Unlike Ar and N<sub>2</sub>, compressed air is inefficient (Fig. S10<sup>†</sup>), which may be attributed to the fact that the air contains a small amount of CO<sub>2</sub> (~300 ppm). On the other hand, the complex solution in both states is very stable in an airtight environment, with no distinct changes after standing at room temperature for at least 30 h (Fig. S11<sup>†</sup>). Both the luminescence intensity and emission color of the DyW<sub>10</sub>/PEO-*b*-PDMAEMA complex can be reversibly switched by alternating CO<sub>2</sub>/Ar treatment for at least five cycles (Fig. 2b), which endows this complex system with the merit of recyclability, making it a more affordable CO<sub>2</sub> detector.

To verify the CO<sub>2</sub>-responsive assembly behavior of DyW<sub>10</sub>/PEO-*b*-PDMAEMA, we used *in situ* small angle X-ray scattering (SAXS), transmission electron microscopy (TEM), and <sup>1</sup>H NMR spectroscopy. The scattering intensity *I*(*q*) of the DyW<sub>10</sub>/copolymer complex at low *q* values became stronger after purging CO<sub>2</sub> into the complex solution (Fig. 3a), supporting the formation of large assembled aggregates. The corresponding pair-distance distribution function *p*(*r*) (Fig. 3b) was deduced by using Generalized Indirect Fourier Transform (GIFT) analysis,<sup>15</sup> and the result shows that the scattering objects have a globular, almost spherical shape with an average diameter of ~12 nm. The TEM image of DyW<sub>10</sub>/PEO-*b*-PDMAEMA assemblies after



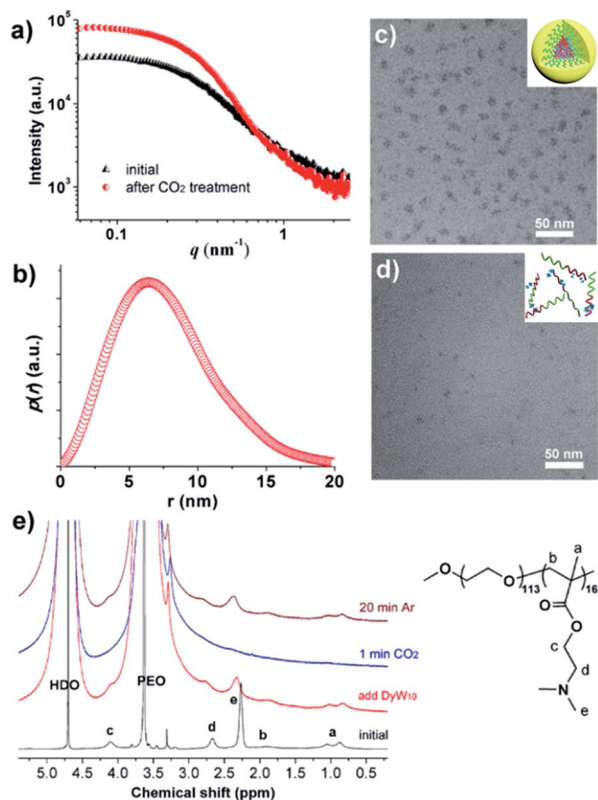


Fig. 3 Characterization of the morphology of the DyW<sub>10</sub>/PEO-*b*-PDMAEMA coassemblies before and after CO<sub>2</sub> treatment. (a) The SAXS pattern obtained for DyW<sub>10</sub>/PEO-*b*-PDMAEMA and (b) the corresponding distance distribution,  $p(r)$ , after treatment with CO<sub>2</sub>; TEM images of DyW<sub>10</sub>/PEO-*b*-PDMAEMA coassemblies after CO<sub>2</sub> (c) and Ar (d) treatment; (e) partial <sup>1</sup>H NMR spectra in D<sub>2</sub>O recorded for the DyW<sub>10</sub>/PEO-*b*-PDMAEMA complex, followed by purging with CO<sub>2</sub> gas, and then degassing CO<sub>2</sub> with Ar.

CO<sub>2</sub> treatment displays spherical micelles with an average diameter of 10 nm with a narrow distribution (Fig. 3c), in good agreement with the SAXS results, while before CO<sub>2</sub> treatment the TEM image displays a lesser amount of small irregular aggregates (Fig. 3d). To probe the PDMAEMA segments participating in the formation of a micellar core with the macroanionic DyW<sub>10</sub>, <sup>1</sup>H NMR spectroscopy was utilized to characterize the signal changes of the PDMAEMA segments in D<sub>2</sub>O solution (Fig. 3e). As expected, compared to the characteristic signals of PDMAEMA at chemical shifts ~2.38, 2.81 and 4.15 ppm recorded for the initial solution, the PDMAEMA signals disappeared completely after CO<sub>2</sub> treatment, indicating that almost all PDMAEMA segments participate in the formation of the coacervate core. Furthermore, the <sup>1</sup>H NMR signals of the PDMAEMA blocks can be restored upon treatment with Ar. All the above results support the co-assembly of DyW<sub>10</sub> and PEO-*b*-PDMAEMA after CO<sub>2</sub> treatment into dense spherical micelles, and the fact that the assembly/disassembly can be reversibly switched by alternating CO<sub>2</sub>/Ar treatment.

To explore the microenvironment variations of the lumiphore DyW<sub>10</sub> before and after purging with CO<sub>2</sub>, further examination of the decay lifetimes of DyW<sub>10</sub>/PEO-*b*-PDMAEMA

coassemblies was carried out (Fig. S12<sup>†</sup>). It is known that the emission of Dy<sup>3+</sup> is highly dependent on coordinated water, due to radiationless deactivation of the <sup>4</sup>F<sub>9/2</sub> excited state through weak coupling with the vibrational states of the high-frequency OH oscillators in the water ligands.<sup>16</sup> In the initial state without CO<sub>2</sub>, three lifetimes could be identified:  $\tau_1 \approx 4.0 \mu\text{s}$  ( $f_1 = 0.366$ ),  $\tau_2 \approx 17.3 \mu\text{s}$  ( $f_2 = 0.201$ ), and  $\tau_3 \approx 59.9 \mu\text{s}$  ( $f_3 = 0.433$ ) ( $f_i$  denotes the fractional contribution to the total fluorescence decay; detailed fitting methods and results are available in Table S1<sup>†</sup>).<sup>17</sup> As the lifetime is correlated to the water molecules coordinated to the Dy<sup>3+</sup> ion, the number of water ligands  $q_{\text{H}_2\text{O}}$  can be estimated to be about 6.2, 1.2, and 0.16, respectively,<sup>18</sup> demonstrating that there are a considerable number of water molecules coordinated to Dy<sup>3+</sup> in the initial state (detailed calculation of  $q_{\text{H}_2\text{O}}$  is given in the ESI<sup>†</sup>). In comparison, after addition of CO<sub>2</sub>, there is only a single long decay lifetime of ~57.5  $\mu\text{s}$  with a  $q_{\text{H}_2\text{O}}$  value of 0.18, which is comparable to that of DyW<sub>10</sub> crystals ( $\tau \approx 58.2 \mu\text{s}$ ,  $q_{\text{H}_2\text{O}} \sim 0.17$ ), indicating there are almost no water molecules coordinated to the Dy<sup>3+</sup> ion. This result further suggests that after CO<sub>2</sub> treatment DyW<sub>10</sub> is located in a relatively hydrophobic environment in the complex core of spherical micelles, where the cationic PDMAEMA segments have strong enough electrostatic affinity to the anionic DyW<sub>10</sub> to replace the water ligands.

What follows is a proposed mechanism of how CO<sub>2</sub> triggers the luminescence chromism. In the initial DyW<sub>10</sub>/PEO-*b*-PDMAEMA dilute solution, the degree of protonation of the PDMAEMA blocks is estimated to be ~61% based on the initial pH value ~7.20 of the DyW<sub>10</sub>/PEO-*b*-PDMAEMA solution (see ESI<sup>†</sup>). The water molecules coordinated to Dy<sup>3+</sup> are only partially replaced by PDMAEMA segments through electrostatic interactions, which in fact lowers the  $D_{4d}$  symmetry of DyW<sub>10</sub> in the solid to  $C_{4v}$ , because the water molecules cannot lie exactly in the reflection plane of the alternating  $S_8$  axis. The  $I_{4F_{9/2} \rightarrow 6H_{13/2}}/I_{4F_{9/2} \rightarrow 6H_{15/2}}$  value ~2.22 as a probe of Dy<sup>3+</sup> symmetry in ambient microenvironments also demonstrates that DyW<sub>10</sub> is located in a relatively asymmetrical microenvironment. In the presence of CO<sub>2</sub>, the *N,N*-dimethylaminoethyl tertiary amino groups of PEO-*b*-PDMAEMA are almost completely converted to positively-charged ammonium bicarbonates (Scheme 1), and the PDMAEMA block is almost fully positively charged with  $\delta \sim 99.8\%$  as estimated from the pH value ~4.80. Consequently, the electrostatic interactions between the cationic copolymer and macroanionic DyW<sub>10</sub> are greatly enhanced and drive their co-assembly into dense spherical micelles consisting of a hydrophobic PDMAEMA/DyW<sub>10</sub> complex core stabilized by a corona of neutral hydrophilic PEO blocks. As DyW<sub>10</sub> is located in the dense core of the micelles, its bound water molecules are almost completely replaced by the protonated PDMAEMA segments, and thus the symmetric microenvironment of DyW<sub>10</sub> is improved as evidenced by a decrease in the  $I_{4F_{9/2} \rightarrow 6H_{13/2}}/I_{4F_{9/2} \rightarrow 6H_{15/2}}$  value to 0.92, which is comparable to that of DyW<sub>10</sub> crystals. As a result, the luminescence intensity is greatly enhanced and the chromism from green to white occurs. On purging with Ar to remove CO<sub>2</sub>, the spherical micelles can disassemble because of the partial deprotonation of PDMAEMA, and consequently the complex solution can be used



for recyclable CO<sub>2</sub> sensing. Its performance does not decline with the number of cycles, because the CO<sub>2</sub>/Ar switching does not cause any salt accumulation or contamination which would destroy the electrostatic assemblies.

## Conclusions

In summary, we have demonstrated a novel supramolecular assay for fluorimetric sensing of carbon dioxide based on a POM/copolymer hybrid complex. PDMAEMA blocks could be protonated by CO<sub>2</sub> leading to electrostatic co-assembly with DyW<sub>10</sub>, and consequently the white emission of DyW<sub>10</sub> is switched on. The fluorimetric characteristics of DyW<sub>10</sub>/PEO-*b*-PDMAEMA coassemblies permit the detection of CO<sub>2</sub> with the merits of simplicity, sensitivity, specificity, interference tolerance, and recyclability. Furthermore, our findings may pave the way to the elaborate design of smart supramolecular materials with complementary functional components.

## Acknowledgements

We would like to thank Prof. Jinying Yuan at Tsinghua University for helpful discussions. This work was supported by the National Natural Science Foundation of China (21322404; 51373001; 21404030), and the Natural Science Foundation of Beijing Municipality (No. 2122024).

## Notes and references

- (a) D. Leaf, H. J. H. Verolme and W. F. Hunt, *Environ. Int.*, 2003, **29**, 303; (b) J. J. Chen and G. B. Pike, *J. Cereb. Blood Flow Metab.*, 2010, **30**, 1094; (c) H. J. Adroque and N. E. Madias, *J. Am. Soc. Nephrol.*, 2010, **21**, 920.
- (a) W. Jin, J. Jiang, Y. Song and C. Bai, *Respir. Physiol. Neurobiol.*, 2012, **180**, 141; (b) J. Zosel, W. Oelssner, M. Decker, G. Gerlach and U. Guth, *Meas. Sci. Technol.*, 2011, **22**, 072001.
- (a) M. E. Lopez, *Anal. Chem.*, 1984, **56**, 2360; (b) H. Suzuki, H. Arakawa, S. Sasaki and I. Karube, *Anal. Chem.*, 1999, **71**, 1737.
- L. Joly, F. Gibert, B. Grouiez, A. Grossel, B. Parvitte, G. Durry and V. Zeninari, *J. Quant. Spectrosc. Radiat. Transfer*, 2008, **109**, 426.
- (a) B. Han, X. Jiang, X. Hou and C. Zheng, *Anal. Chem.*, 2014, **86**, 936; (b) V. M. Vorotyntsev, G. M. Mochalov and I. V. Baranova, *J. Anal. Chem.*, 2013, **68**, 152.
- (a) Q. Xu, S. Lee, Y. Cho, M. H. Kim, J. Bouffard and J. Yoon, *J. Am. Chem. Soc.*, 2013, **135**, 17751; (b) Y. Ma, H. Xu, Y. Zeng, C.-L. Ho, C.-H. Chui, Q. Zhao, W. Huang and W.-Y. Wong, *J. Mater. Chem. C*, 2015, **3**, 66.
- (a) Y. Ma and L.-Y. L. Yung, *Anal. Chem.*, 2014, **86**, 2429; (b) J. J. Gassensmith, J. Y. Kim, J. M. Holcroft, O. K. Farha, J. F. Stoddart, J. T. Hupp and N. C. Jeong, *J. Am. Chem. Soc.*, 2014, **136**, 8277; (c) E. Climent, A. Agostini, M. E. Moragues, R. Martinez-Manez, F. Sancenon, T. Pardo and M. D. Marcos, *Chem.–Eur. J.*, 2013, **19**, 17301.
- (a) Z. Guo, N. R. Song, J. H. Moon, M. Kim, E. J. Jun, J. Choi, J. Y. Lee, C. W. Bielawski, J. L. Sessler and J. Yoon, *J. Am. Chem. Soc.*, 2012, **134**, 17846; (b) Y. Liu, Y. Tang, N. N. Barashkov, I. S. Irgibaeva, J. W. Y. Lam, R. Hu, D. Birimzhanova, Y. Yu and B. Z. Tang, *J. Am. Chem. Soc.*, 2010, **132**, 13951; (c) L. Q. Xu, B. Zhang, M. Sun, L. Hong, K.-G. Neoh, E.-T. Kang and G. D. Fu, *J. Mater. Chem. A*, 2013, **1**, 1207; (d) T. A. Darwish, R. A. Evans, M. James and T. L. Hanley, *Chem.–Eur. J.*, 2011, **17**, 11399; (e) J. Guo, N. Wang, J. Wu, Q. Ye, C. Zhang, X.-H. Xing and J. Yuan, *J. Mater. Chem. B*, 2014, **2**, 437; (f) T. Tian, X. Chen, H. Li, Y. Wang, L. Guo and L. Jiang, *Analyst*, 2013, **138**, 991.
- C. M. Rudzinski, A. M. Young and D. G. Nocera, *J. Am. Chem. Soc.*, 2002, **124**, 1723.
- (a) J. Zhang, Y. Liu, Y. Li, H. Zhao and X. Wan, *Angew. Chem., Int. Ed.*, 2012, **51**, 4598; (b) H. Wei, S. Du, Y. Liu, H. Zhao, C. Chen, Z. Li, J. Lin, Y. Zhang, J. Zhang and X. Wan, *Chem. Commun.*, 2014, **50**, 1447; (c) Y. Liu, H. Zhao, H. Wei, N. Shi, J. Zhang and X. Wan, *J. Inorg. Organomet. Polym. Mater.*, 2015, **25**, 126.
- (a) K. Sawada and T. Yamase, *Acta Crystallogr., Sect. C: Cryst. Struct. Commun.*, 2002, **58**, i149; (b) K. Binnemans, *Chem. Rev.*, 2009, **109**, 4283; (c) T. Yamase, *Chem. Rev.*, 1998, **98**, 307; (d) R. Ballardini, Q. G. Mulazzani, M. Venturi, F. Bolletta and V. Balzani, *Inorg. Chem.*, 1984, **23**, 300.
- C. H. Liang, L. G. Teoh, K. T. Liu and Y. S. Chang, *J. Alloys Compd.*, 2012, **517**, 9.
- H. Wei, N. Shi, J. Zhang, Y. Guan, J. Zhang and X. Wan, *Chem. Commun.*, 2014, **50**, 9333.
- D. Han, X. Tong, O. Boissiere and Y. Zhao, *ACS Macro Lett.*, 2012, **1**, 57.
- (a) D. Lof, M. Tomsic, O. Glatter, G. Fritz-Popovski and K. Schillen, *J. Phys. Chem. B*, 2009, **113**, 5478; (b) B. Weyerich, J. Brunner-Popela and O. Glatter, *J. Appl. Crystallogr.*, 1999, **32**, 197.
- G. Stein and E. Wurzburg, *J. Chem. Phys.*, 1975, **62**, 208.
- J. R. Lakowicz, *Principles of Fluorescence Spectroscopy*, Springer, Berlin, 3rd edn, 2006, p. 101.
- C. D. Hall and N. W. Sharpe, *J. Photochem. Photobiol., A*, 1990, **52**, 363.

